U. S.   A R M Y

TRANSPORTATION RESEARCH COMMAND

FORT EUSTIS, VIRGINIA

TCREC TECHNICAL REPORT 61-124

AN INVESTIGATION OF A DIGITAL COMPUTER METHOD OF DETERMINING THE OPTIMUM DESIGN PARAMETER OF SHROUDED PROPELLERS

Task 9R38-11-009-12

Contract DA 44-177-TC-402

Job Order No. 4

October 1961

prepared by :

GEORGIA INSTITUTE OF TECHNOLOGY
Atlanta, Georgia

DISCLAIMER NOTICE

Task 9R38-11-009-12

Contract DA 44-177-TC-402

Job Order No. 4

October, 1961

AN INVESTIGATION OF A DIGITAL COMPUTER METHOD OF

DETERMINING THE OPTIMUM DESIGN PARAMETERS OF

SHROUDED PROPELLERS

Prepared by

Engineering Experiment Station

Georgia Institute of Technology

Atlanta 13, Georgia

for

U. S. Army Transportation Research Command

Fort Eustis, Virginia

PREFACE

This report is one of a series presenting the results of research in the field of shrouded propeller aerodynamics, performed under contract for the U. S. Army Transportation Research Command, Fort Eustis, Virginia.

This work, performed by Dr. Gray and his associates at the Engineering Experiment Station, Georgia Institute of Technology, is a follow-on of the work reported in U. S. Army Transportation Research Command TREC Report 60-44. The present report devotes itself to the application and refinement of the digital computer method for the determination of optimum blade-bound strength distributions.

The report has been reviewed by the U. S. Army Transportation Research Command and is considered technically sound. The report is published for the exchange of information and the stimulation of ideas.

ROBERT R. GRAHAM

USATRECOM Project Engineer

EARL A. WIRTH
CWO-4   USA
Adjutant

FOREWORD

The investigation described in this report was undertaken by the Engineering Experiment Station, Georgia Institute of Technology, Atlanta, Georgia, for the VTOL/STOL Design Criteria Branch of the Aero-Mechanics Division, U. S. Army Transportation Research Command, Fort Eustis, Virginia. Dr. Robin B. Gray of the Georgia Institute of Technology was project director, and Mr. James Scheiman and Captain Dean E. Wright of the VTOL/STOL Design Criteria Branch of the Aero-Mechanics Division were the administrative representatives for TRECOM. The contract period extended from 7 December 1960 to 7 September 1961.

The author wishes to extend his appreciation to Prof. Walter Castles, Jr., of the Georgia Institute of Technology for his comments and suggestions during the course of the investigation and to Mr. James C. Stein, of the Rich Electronic Computer Center, Engineering Experiment Station for his assistance in preparing the computer program.

CONTENTS

LIST OF SYMBOLS

A_n coefficients of cosine terms appearing in Fourier series representation of blade bound vortex distribution

b   number of propeller blades

B_n coefficients of sine terms appearing in Fourier series representation of blade bound vortex distribution

H   geometric pitch of the vortex filaments forming the sheet

$K(x)$ nondimensional blade bound vortex distribution,

$$K(x) = \frac{b \; \Gamma}{2\pi R_o \; w \; \tan \varphi_o}$$

L   axial spacing between successive inner helical vortex sheets

m   subscript denoting particular finite strength vortex filament replacing a segment of the vortex sheet

M   number of finite strength vortex filaments used to approximate the wake vortex sheets

r   radial co-ordinate defining calculating point

r'   radial co-ordinate defining element of vortex filament

$\overline{r}$ nondimensional radius of calculating point, $\dfrac{r}{R_o}$

$\overline{r}'$ nondimensional radius of element of vortex filament, $\dfrac{r'}{R_o}$

R   propeller blade radius

R_o ultimate wake radius

ds'   length of elemental vortex filament

u_r radial induced velocity component

u_x, u_y, u_z induced velocity components parallel to the x-, y-, and z-axes, respectively

u_ζ induced velocity component that is normal to both the vortex filament and the radial induced velocity component

vii

u_ξ induced velocity component in the direction of the vortex filament and normal to the radial induced velocity component

V_i induced velocity

w parameter describing the apparent axial velocity of the wake vortex system

x,y,z Cartesian co-ordinates defining the point at which the velocity components are desired. The z-axis and the axis of the vortex system coincide. The positive z-direction is in the direction of advance of the vortex system.

x',y',z' Cartesian co-ordinates defining the position of the vortex element ds'

$\bar{x}$ nondimensional radius $\dfrac{\bar{r}}{\tan \varphi_o}$

$\bar{x}'$ nondimensional radius of vortex filament $\dfrac{\bar{r}'}{\tan \varphi_o}$

x'_m Cartesian co-ordinate of particular vortex filament

z'_o shortest axial distance between the x-axis and the intersection of the vortex filament with the xz-plane

β angle between the normal to the vortex element ds' and the displacement vector $\bar{P}$ from ds' to the point; measured in the plane determined by $d\bar{s}'$ and $\bar{P}$

γ vortex sheet strength

Γ blade bound vortex strength

ζ helical co-ordinate measured normal to vortex filament and radial co-ordinate

κ strength of finite vortex filament

λ tangent of the helix angle of the blade tip vortex filament

ξ helical co-ordinate measured along vortex filament

P distance from the element ds' to the point under consideration

φ helix pitch angle of the sheet at the point where the induced velocity components are to be computed

φ' helix pitch angle of vortex filament

φ_o helix pitch angle of the vortex filaments forming the wake boundary

ψ angular co-ordinate of cylindrical co-ordinate system

ψ' angular co-ordinate defining location of element of vortex filament

ψ'' defined as $\quad - (\psi_o - \psi')$

ψ_o defined as $\quad (\dfrac{z}{R_o} - \dfrac{z_o'}{R_o})/\tan \varphi_o$

ψ_s defined as $\quad (\psi_o - \psi)$

SUMMARY

A digital computer method of determining the optimum design para-
meters of lightly loaded shrouded propellers is presented. For such a
case the geometry of the vortex wake may be ideally described as a heli-
cal sheet of equal-pitch vortex filaments arising from each blade trail-
ing edge and a right circular boundary sheet composed of equal-pitch
helical filaments arising at the shroud trailing edge. The optimum con-
dition for light loading requires that this wake vortex pattern move as
a rigid body. This pattern of distributed vorticity is arbitrarily re-
placed with a finite number of finite, but unknown strength, vortex fila-
ments. Using the Biot-Savart relation, an expression for the velocity
components associated with each filament is obtained. Applying the
boundary conditions to these sets of equations results in a set of si-
multaneous equations in terms of the unknown filament strengths. The
blade bound vortex distribution obtained from the simultaneous solution
is compared with the measurements previously obtained from potential tank
models of a two- and four-bladed shrouded propeller. It is concluded
that this digital computer method yields results that are adequate for
design purposes, and it is recommended that this method be used instead of
the potential tank method for obtaining the necessary charts and tables
covering the range of design parameters for shrouded propellers.

1

CONCLUSIONS

The digital computer method of determining the optimum blade bound vortex strength distribution of shrouded propellers presented herein yields results very similar to those obtained from the potential tank models. Of the two approaches to the problem, it is concluded that the digital computer method is the more accurate and efficient. The use of a Fourier series representation of the blade bound vortex distribution was proven to be advantageous, primarily as an aid in presenting the results for design purposes.

Although the method was developed for the lightly loaded case, it is believed that the approach with certain modifications to the boundary conditions may be employed to determine the optimum blade bound vortex strength for heavily loaded shrouded propellers.

RECOMMENDATIONS

It is recommended that the digital computer method of determining the optimum blade bound vortex strength distributions of shrouded propellers be used instead of the potential tank method in any extension of the present work. In addition, the use of a Fourier series representation of the bound vortex strength will reduce the number of charts and tables required to cover the range of design variables.

Inasmuch as the present method was developed for lightly loaded, shrouded propellers, it is believed that a heavily loaded theory would be more advantageous. It is recommended that any extension of the present work be for the heavily loaded case.

INTRODUCTION

The mathematical description of fluid flow fields associated with lifting surfaces has often been made less difficult by the introduction of the bound vortex concept and its accompanying pattern of vortex sheets. This has been particularly true for those cases of three-dimensional wings and for propellers in which the geometry of the vortex patterns could be ascertained beforehand. If the geometry is known and the vortex filament and sheet strengths are unknown, then the solution is, in theory, straightforward, and two classical avenues may be followed. One method involves the obtaining of a solution to Laplace's equation in terms of the velocity potential which satisfies the boundary conditions of the particular problem. By further consideration of the direct analogy that exists between the electrical and velocity potentials, potential tank models may be used to obtain solutions for those cases which are not mathematically tractable. In addition, of course, a solution may be reached through numerical procedures and approximations. A second method makes use of the Biot-Savart equation which is a differential relation between the incremental velocity at a point associated with an incremental length of vortex filament and its strength and geometry. The integration of this expression usually involves numerical procedures and approximations and also the satisfaction of certain boundary conditions.

In recent years, a number of prototype and test-bed aircraft having VTOL/STOL capabilities have been constructed that have used the shrouded or ducted propeller for propulsion and sustentation. The results

of the tests of these aircraft have indicated a need for a better under-

standing of the effects of the shroud or duct on propeller performance.

Several theoretical investigations have been directed toward determining

the necessary optimum design parameters of propellers operating in ducts.

One analysis[1] considered a lightly loaded propeller having a minimum ki-

netic energy loss operating in a circular duct of constant diameter and

of infinite or semi-infinite length. A series-type solution of Laplace's

equation for the velocity potential with the necessary boundary condi-

tions was obtained. The coefficients appearing in the solution were de-

termined by a standard method of successive approximations. The bound

vortex strength distribution was determined, and the increase in this

quantity and the thrust increment over that of a free propeller were pre-

sented in tables for a propeller operating in a duct with zero-tip clear-

ance. The tables presented the values for three-, four-, five-, and six-

bladed shrouded propellers operating at advance ratios of one-sixth to

two-thirds.

The potential tank technique of determining the optimum design

parameters of shrouded propellers has been developed and presented[2] by

the author of this report. In developing the technique, potential models

were constructed of the ultimate wake of a two- and four-bladed shrouded

---

[1]A. J. Tachmindji, The Potential Problem of the Optimum Propeller

with Finite Number of Blades Operating in a Cylindrical Duct, David Taylor

Model Basin, Report No. 1228, July, 1958.

[2]R. B. Gray, An Investigation of an Approach to the Problem of

Determining the Optimum Design of Shrouded Propellers, U. S. Army Trans-

portation Research Command, Report TREC 60-44, May, 1960.

5

propeller operating at an advance ratio of 1.356 and the measurements were made on, and the data presented for, these models. It was concluded that the approach yielded answers suitable for design prupoees but that the model construction was difficult and time consuming. A second method of determining the necessary design parameters involving the digital computer integration of the Biot-Savart relation was also presented in that report. Although the results of the digital computer analysis were inconclusive due to limitations of time and funds, it was recommended that the computer approach be pursued to its conclusions. It is the results of the extension of this digital computer analysis that are presented in this report.

6

ANALYSIS OF PROBLEM

For the case of the lightly loaded shrouded propeller, the geometry of the ultimate vortex wake may be easily described, and hence the well-established vortex theories[3] may be applied in a straightforward manner. Here, the term "lightly loaded" should be interpreted as yielding induced velocities that are negligibly small in comparison with the free-stream velocity and the local blade rotational velocities. In addition, it is implied that the wake has reached its ultimate configuration at the shroud trailing edge and that a vortex filament shed at a nondimensional blade station remains at that nondimensional radius with respect to the local wake radius. The resulting vortex pattern has been discussed in Appendix I of Gray's Report[2] and its geometry is assumed to be specified by the free-stream velocity and the blade rotational velocity. Thus the vortex system is assumed to be composed of two parts. One part is formed of equal geometric-pitch helical filaments extending from each blade trailing edge downstream to infinity. The second part is a circular cylinder of equal-pitch helical vortex filaments extending from the shroud trailing edge downstream to infinity and enclosing the helical sheets shed from the blades. There are the same number of helical lines of intersection of these two parts as there are number of blades.

As was discussed in Gray's Report[2], the optimum condition requires

[3]Horace Lamb, Hydrodynamics, Sixth Edition, Chap. VII, Dover Publications, New York, 1945.

[2]Gray, op. cit. ante page 5.

7

that in the ultimate wake this vortex system must appear to move as a
rigid body; that is, without distortion. This requirement yields the
boundary conditions both on the motion of the vortex filaments and on the
blade bound vortex strength distribution. For instance, if no distortion
of the vortex pattern is to occur, then the radial component of the in-
duced velocity must be zero for all points on the vortex sheet and, in
addition, the component of induced velocity that is normal to the helical
filaments and the radial co-ordinate must be such that its axial component
is identical for all points on the vortex sheets. The induced velocity
component in the direction of the filament is immaterial.

The relationship between the induced velocity, the vortex filament
strength, and the vortex geometry is given by the Biot-Savart relation
which states that

$$dV_i = \frac{\kappa}{4\pi} \frac{\cos \beta \ ds'}{P^2} \tag{1}$$

where dV_i is the increment at an arbitrary point of the induced
velocity that is associated with a vortex element of
length ds'.

κ is the strength of the vortex element.

β is the angle between the normal to the element ds'
and the displacement vector, $\bar{P}$ from ds' to the
point; measured in the plane determined by $\bar{ds}'$ and
$\bar{P}$.

ds' is the length of the elemental vortex filament.

P is the distance from element ds' to the point under
consideration.

The equations for the velocity components associated with an isolated re-
entrant vortex filament in Cartesian co-ordinates are given on page 211 of

8

Lamb's <u>Hydrodynamics</u> and are repeated below.

$$u_x = \frac{\kappa}{4\pi} \int \left\{ \frac{dy'}{ds'} \left(\frac{z - z'}{P}\right) - \frac{dz'}{ds'} \left(\frac{y - y'}{P}\right) \right\} \frac{ds'}{P^2} \tag{2a}$$

$$u_y = \frac{\kappa}{4\pi} \int \left\{ \frac{dz'}{ds'} \left(\frac{x - x'}{P}\right) - \frac{dx'}{dz'} \left(\frac{z - z'}{P}\right) \right\} \frac{ds'}{P^2} \tag{2b}$$

$$u_z = \frac{\kappa}{4\pi} \int \left\{ \frac{dx'}{ds'} \left(\frac{y - y'}{P}\right) - \frac{dy'}{ds'} \left(\frac{x - x'}{P}\right) \right\} \frac{ds'}{P^2} \tag{2c}$$

where, as shown in Figure 1

x,y,z are the Cartesian co-ordinates defining the point at which the velocity components are desired. The z-axis and the axis of the vortex system coincide. The positive z-direction is in the direction of advance of the vortex system.

x',y',z' are the Cartesian co-ordinates defining the position of the vortex element ds'.

u_x, u_y, u_z are the induced velocity components parallel to the x-, y-, and z-Axes, respectively.

$$P = \left\{ (x - x')^2 + (y - y')^2 + (z - z')^2 \right\}^{\frac{1}{2}} \tag{3}$$

The helical filament may be more easily described in cylindrical co-ordinates (r, ψ, z) so that the following transformation is made.

$$x = r \cos \psi$$
$$y = r \sin \psi$$
$$z = z$$

9
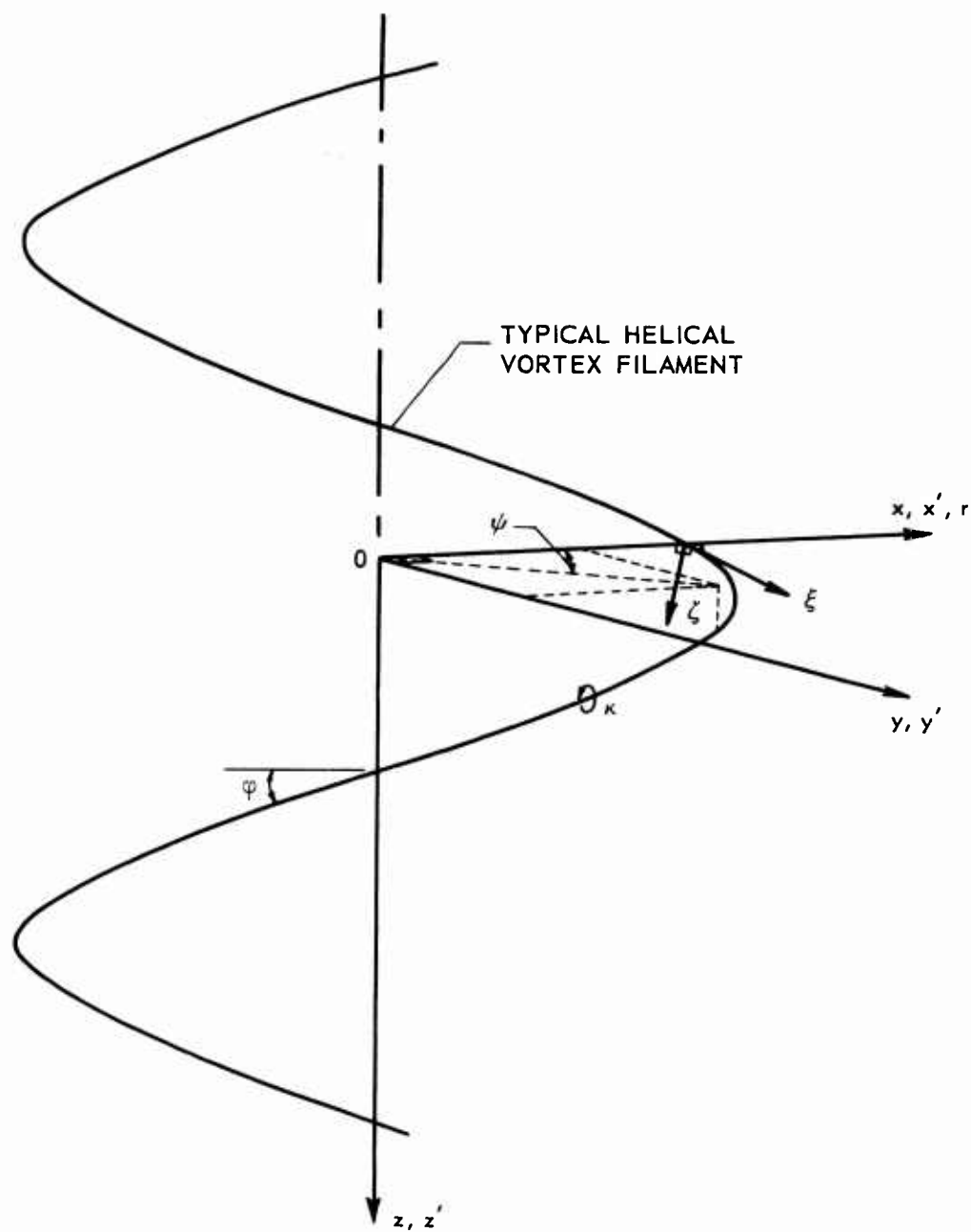
Figure 1. Coordinate Systems.

10

$$x' = r' \cos \psi^r$$

$$y' = r' \sin \psi'$$

$$z' = z_o' + r' \psi' \tan \varphi'$$

$$s' = r' \psi' \sec \varphi'$$

where φ' is the helix pitch angle of the vortex filament.

z_o' is the shortest axial distance between the x-axis and the intersection of the vortex filament with the xz-plane.

The boundary conditions are more conveniently expressed in terms of the velocity components along and perpendicular to the vortex sheet filaments. Thus,

$$u_r = u_x \cos \psi + u_y \sin \psi$$

$$u_\xi = (u_y \cos \psi - u_x \sin \psi) \cos \varphi + u_z \sin \varphi$$

$$u_\zeta = u_z \cos \varphi - (u_y \cos \psi - u_x \sin \psi) \sin \varphi$$

where u_r is the radial induced velocity component.

u_ξ is the induced velocity component in the direction of the vortex filament and normal to the radial component.

u_ζ is the induced velocity component that is normal to both the vortex filament and the radial component.

φ is the helix pitch angle of the sheet at the point where the induced velocity components are to be computed.

Performing the above transformations yields the following expressions for the induced velocity components associated with an infinite length, helical vortex filament.

11

$$u_r = \frac{\kappa}{4\pi} \int_{-\infty}^{\infty} \left\{ r'^2 \tan \varphi' \sin (\psi' - \psi) + \right.$$

$$\left. r' \left[z - z_0' - r' \psi' \tan \varphi' \right] \cos (\psi' - \psi) \right\} \frac{d\psi'}{P^3} \qquad (4a)$$

$$u_\xi = \frac{\kappa}{4\pi} \int_{-\infty}^{\infty} \left\{ \left[r' \tan \varphi' \left[r - r' \cos (\psi' - \psi) \right] + \right. \right.$$

$$\left. r'(z - z_0' - r' \psi' \tan \varphi') \sin (\psi' - \psi) \right] \cos \varphi +$$

$$\left. \left[r'^2 - rr' \cos (\psi' - \psi) \right] \sin \varphi \right\} \frac{d\psi'}{P^3} \qquad (4b)$$

$$u_\zeta = \frac{\kappa}{4\pi} \int_{-\infty}^{\infty} \left\{ \left[r'^2 - rr' \cos (\psi' - \psi) \right] \cos \varphi - \right.$$

$$\left[r' \tan \varphi' \left[r - r' \cos (\psi' - \psi) \right] + \right.$$

$$\left. r'(z - z_0' - r' \psi' \tan \varphi') \sin (\psi' - \psi) \right] \sin \varphi \right\} \frac{d\psi'}{P^3} \qquad (4c)$$

$$\text{where } P = \left\{ r^2 + r'^2 - 2rr' \cos (\psi' - \psi) + (z - z_0' - r' \psi' \tan \varphi')^2 \right\}^{\frac{1}{2}} \qquad (5)$$

In order to obtain the total velocity components for the entire pattern, Equation (4) must be integrated over the entire vortex sheet. As far as is known, a solution to these equations in terms of the elementary functions has not been determined so that numerical means must be used. Thus, the vortex sheet is arbitrarily divided into a finite number

12

of equal-width segments and each segment is replaced by a finite strength
vortex filament. The boundary conditions previously prescribed for the
motion of the sheets must be applied to a finite number of points on the
sheet other than those which would lie on the filaments in order that
Equation (5) will remain greater than zero and the integrands of Equation
(4) will remain finite. For this reason, the calculating points for this
analysis are chosen on the sheet and midway between the vortex filaments;
i.e., the points separating two consecutive vortex segments. As pointed
out before, the strengths of these vortex filaments are unknown. There-
fore, for each calculating point, an equation for each induced velocity
component is obtained in terms of the unknown vortex strengths. The
boundary conditions on the radial and normal components of induced velo-
city for points on the vortex sheet are

$$u_r = 0 \tag{6}$$

$$u_\zeta = w \cos \varphi \tag{7}$$

where w is the parameter describing the apparent axial motion of the
wake vortex system. For "M" vortex filaments, the nondimensional equa-
tions are

$$\sum_{m=1}^{M} \left(\frac{\kappa_m}{4\pi R_o w}\right) \int_{-\infty}^{\infty} \left\{ \bar{r}' \tan \varphi_o \sin (\psi' - \psi) + \right.$$

$$\left. \bar{r}' \left[\frac{z}{R_o} - \frac{z_o'}{R_o} - \psi' \tan \varphi_o\right] \cos (\psi' - \psi) \right\} \frac{d\psi'}{P_m^3} = 0 \tag{8}$$

13

$$\sum_{m=1}^{M} \left(\frac{\kappa_m}{4\pi R_o w}\right) \int_{-\infty}^{\infty} \left\{ (\overline{r}'^2 - \tan^2 \varphi_o) + \left(\frac{\overline{r}'}{\overline{r}} \tan^2 \varphi_o - \overline{rr}'\right) \cos (\psi' - \psi) - \right.$$

$$\left. \frac{\overline{r}'}{\overline{r}} \left[\frac{z}{R_o} - \frac{z_o'}{R_o} - \psi' \tan \varphi_o\right] \tan \varphi_o \sin (\psi' - \psi) \right\}_m \frac{d\psi'}{P_m^3} = 1.0 \qquad (9)$$

where

$$\overline{r}' = \frac{r'}{R_o}$$

$$\overline{r} = \frac{r}{R_o}$$

$$\tan \varphi_o = \overline{r}' \tan \varphi' = \overline{r} \tan \varphi$$

$$P_m = \left\{ \overline{r}^2 + \overline{r}'^2 - 2\overline{rr}' \cos (\psi' - \psi) + \left[\frac{z}{R_o} - \frac{z_o'}{R_o} - \psi' \tan \varphi_o \right]^2 \right\}^{\frac{1}{2}} \qquad (10)$$

φ_o is the helix pitch angle of the vortex filaments forming the wake boundary.

R_o is the wake radius.

Forms more suitable both for computing purposes and for recognizing repeating coefficients in the sets of equations are as follows.

$$\sum_{m=1}^{M} \left(\frac{\kappa_m}{2\pi R_o w \tan \varphi_o}\right) \left(\frac{\overline{x}'_m}{2}\right) \int_{o}^{\infty} \left\{ (\cos \psi_s + \psi'' \sin \psi_s) \frac{\sin \psi''}{P_1} + \right.$$

$$(\sin \psi_s - \psi'' \cos \psi_s) \frac{\cos \psi''}{P_1} + (\psi'' \sin \psi_s - \cos \psi_s) \frac{\sin \psi''}{P_2} +$$

$$\left. (\sin \psi_s + \psi'' \cos \psi_s) \frac{\cos \psi''}{P_2} \right\}_m d\psi'' = 0 \qquad (11)$$

14

$$\sum_{m=1}^{M} \left(\frac{\kappa_m}{2\pi R_o \, w \, \tan \varphi_o}\right) \left(\frac{1}{2}\right) \int_o^\infty \left\{ \frac{b_3}{P_1} + (b_4 \cos \psi_s + b_5 \, \psi'' \sin \psi_s) \frac{\cos \psi''}{P_1} + \right.$$

$$(b_5 \, \psi'' \cos \psi_s - b_4 \sin \psi_s) \frac{\sin \psi''}{P_1} +$$

$$\frac{b_3}{P_2} + (b_4 \cos \psi_s - b_5 \, \psi'' \sin \psi_s) \frac{\cos \psi''}{P_2} +$$

$$\left. (b_5 \, \psi'' \cos \psi_s + b_4 \sin \psi_s) \frac{\sin \psi''}{P_2} \right\}_m \, d\psi'' = 1.0 \quad (12)$$

where $P_1 = \left\{ b_1 - b_2(\cos \psi_s \cos \psi'' - \sin \psi_s \sin \psi'') + \psi''^2 \right\}^{3/2}$

$P_2 = \left\{ b_1 - b_2(\cos \psi_s \cos \psi'' + \sin \psi_s \sin \psi'') + \psi''^2 \right\}^{3/2}$

$\overline{x} = \dfrac{\overline{r}}{\tan \varphi_o}$

$\overline{x}' = \dfrac{\overline{r}'}{\tan \varphi_o}$

$\psi'' = -(\psi_o - \psi')$

$\psi_o = \left(\dfrac{z}{R_o} - \dfrac{z_o'}{R_o}\right) / \tan \varphi_o$

$\psi_s = \psi_o - \psi$

$b_1 = \overline{x}^2 + \overline{x}'^2$

$b_2 = 2 \, \overline{x} \, \overline{x}'$

15

$$b_3 = \overline{x}'^2 - 1$$

$$b_4 = \frac{\overline{x}'}{\overline{x}} - \overline{x}\,\overline{x}'$$

$$b_5 = \frac{\overline{x}'}{\overline{x}}$$

Inspection of the integrand of Equation (11) shows that for a boundary sheet strength distribution symmetrical about its lines of intersection with the inner helical sheets, the radial velocity due to the entire system is zero for all points on the inner sheets. Therefore the radial velocity boundary condition need be satisfied only for points on the boundary sheet. In addition, for the pairs of calculating points on the boundary sheet symmetrically situated with respect to the line of intersection, the equations obtained from (11) are identical. Thus, the number of points at which the radial boundary condition must be satisfied is reduced to half the number of points chosen on the wake boundary vortex sheet if these points are symmetrically disposed about a line of inter-section.

It is only for the lightly loaded case (i.e., vanishingly small induced velocities) that the assumption of equal geometric pitch for all vortex filaments holds. For cases of finite loadings, such an assumption results in an incompatibility between the boundary vortex sheet strength and the discontinuity in the normal induced velocity component u_ζ across the wake boundary sheet. Therefore, for the lightly loaded case, Equation (12) need be satisfied only for those points lying on the inner helical sheet as this is the condition that determines the optimum load-

16

ing. The axial induced velocity boundary condition should not be applied to the vortex filaments in the wake boundary sheet. Thus, the set of equations resulting from (12) is reduced to a number equal to the number of calculating points on the inner helical sheet.

The integrals of Equations (11) and (12) are evaluated numerically on a digital computer, yielding a set of simultaneous equations, one less than the number of unknowns. The last required equation is discussed at the end of this section.

It is now in order to discuss the boundary conditions on the blade bound vortex strength distribution. Considering first the inner helical vortex sheet, the local strength of this sheet in the ultimate wake is related to the change in blade bound vortex strength at the same non-dimensional radial station by the following relation

$$\gamma = (\frac{d \Gamma}{d r}) \tag{13}$$

where $\Gamma = \Gamma(r)$ is the blade bound vortex strength distribution.

$\gamma = \gamma(r)$ is the vortex sheet strength.

For the finite strength filaments

$$\kappa_m = \Gamma(r_2) - \Gamma(r_1) = \int_{r_1}^{r_2} (\frac{d \Gamma}{d r}) dr \tag{14}$$

where the helical sheet between the radii r_1 and r_2 has been replaced by a single vortex filament of strength κ and located midway between r_1 and r_2. The blade bound vortex strength must be zero at the blade root. At the intersection of the inner helical sheet with the boundary

17

sheet, there can be no radial velocities otherwise there would be a continual distortion of the vortex pattern. Since the radial velocities are zero, there is no discontinuity in radial velocity at the tip of the helical sheet as the sheet is crossed so that by the Helmholtz theorems, the sheet strength at this point is zero. Thus, the blade bound vortex strength at the blade tip is constant or $(\frac{d\,\Gamma}{d\,r})_R = 0$.

These boundary conditions may be easily applied by assuming a Fourier series representation of the blade bound vortex strength in the following nondimensional form.

$$\frac{\Gamma}{2\pi R_o\; w\; \tan\,\varphi_o} = A_o + \sum_{m=1}^{\infty} A_n \cos\frac{m\pi}{2}\,\bar{r} + \sum_{m=1}^{\infty} B_n \sin\frac{m\pi}{2}\,\bar{r} \qquad (15)$$

For $\bar{r} = 0;\; \Gamma = 0$ so that $A_o = A_1 = A_2 = ---- = A_n = 0$.

For $\bar{r} = 1.0;\; \frac{d\,\Gamma}{d\,r} = 0$ so that $B_2 = B_4 = B_6 = ---- = 0$.

Thus, the bound vortex strength may be represented by the infinite series

$$\frac{\Gamma}{2\pi R_\cap\; w\; \tan\,\varphi_o} = B_1 \sin\frac{\pi}{2}\,\bar{r} + B_3 \sin\frac{3\pi}{2}\,\bar{r} + B_5 \sin\frac{5\pi}{2}\,\bar{r} + ---- \qquad (16)$$

The nondimensional vortex filament strength which replaces the mth segment of the sheet is then the difference in the values obtained from Equation (16) at each end of the segment. (It is to be noted that in using Equation (16) in the ultimate wake, $\bar{r} = \frac{r}{R_o}$; while at the propeller blade, $\bar{r} = \frac{r}{R}$.)

For the lightly loaded case, there are no requirements on the vortex strength distribution of the boundary sheet. It is to be noted, however, that the boundary sheet strength is periodic, having a period of

$\frac{2\pi R_o \tan \varphi_o}{b}$. In addition, it is symmetrical about its line of inter-

section with the inner helical sheet and also about the midpoint between

adjacent inner sheets. In a manner similar to that of the inner sheet and

for computational purposes, one period of the boundary sheet is divided

into equal-width segments and each segment is replaced by a helical vortex

filament of finite strength and located at its midpoint.

There is one additional important requirement and that is that the

summation of the vortex filament strengths have to be zero according to

the Helmholtz theorems, or, in other words, the line integral of the

velocity along a closed path completely encircling the wake must be zero.

This yields the one additional equation required for the simultaneous

solution.

COMPUTING PROCEDURES

For the particular problem under consideration, it was convenient to divide the vortex system into two parts and to further subdivide each part into an equal number of equal-width segments. The inner helical vortex sheet was thus divided into 10 equal-width segments, starting at $\bar{r}' = 0.0$. Each segment was replaced at its midpoint by a helical vortex filament of finite, but unknown strength, starting at $\bar{r}' = 0.05$ and ending at the $\bar{r}' = 0.95$ station with $z' = 0.0$. The calculating points were chosen at the ends of the segments, beginning at $\bar{r} = 0.0$ and ending with $\bar{r} = 0.9$. A portion of the boundary sheet was also divided into 10 equal-width segments and each segment was replaced by a helical vortex filament as before. Since the boundary sheet strength distribution will be periodic in the axial co-ordinate, the portion that was considered extended from the midpoint between adjacent inner helical sheets and on the wake boundary to the next midpoint in the negative axial direction. The inner sheet spacing is given by

$$L = \frac{H}{b} = \frac{2\pi R_o \tan \varphi_o}{b} \tag{17}$$

or nondimensionally

$$\frac{L}{R_o} = \frac{2\pi \tan \varphi_o}{b} \tag{18}$$

20

where   L   is the axial spacing between successive inner helical
vortex sheets.

H   is the geometric pitch of the vortex filaments forming
the sheet.

b   is the number of blades in the propeller.

Thus, the wake boundary filaments were chosen to lie at $z' = \pm \frac{0.05H}{b}$; $\pm \frac{0.15H}{b}$; ----- ; $\pm \frac{0.45H}{b}$ with $\overline{r}' = 1.0$. The calculating points were chosen midway between the filaments as follows: $z = \pm \frac{0.1H}{b}$; $\pm \frac{0.2H}{b}$; ----- ; $+ \frac{0.5H}{b}$ with $\overline{r} = 1.0$. For the two-bladed propeller wake; $\psi = 0$; π radians. For the four-bladed propeller wake; $\psi = 0$; $\frac{\pi}{2}$; π ; $\frac{3\pi}{2}$ radians. In the example considered in this report, $\tan \varphi_0 = 1.356$.

For given r, z, and ψ, the integrals of Equations (11) and (12) may be evaluated numerically on a digital computer for each vortex filament, thereby yielding for this case of 20 filaments, 40 equations with the nondimensional filament strengths being the 20 unknowns. The intervals $\Delta\psi''$ used in the Simpson's rule integration were determined in the following manner: First, an interval of 0 to π radians was chosen; the integrands were evaluated every 15° of this interval, the Simpson's rule integration was performed, and the result was recorded. The 15° interval was then halved to 7.5°, the above procedure was repeated and the result was compared with the previous result. This process of halving the interval was repeated until the results compared within three units in the sixth significant figure. When this occurred, the next interval, π to 2π radians was chosen and the process repeated. The upper limit on ψ'' was determined by comparing the result of the numerical integration after each π interval with the previous result.

When these computations compared within three units in the fifth significant figure, the integration for that filament was terminated.

As was pointed out in the previous section, the calculation of all the coefficients appearing in the sets of equations was not necessary. For the cases considered herein, Equation (11) yielded four equations for satisfying the radial induced velocity component on the wake boundary (note that point $z = \pm \frac{0.5H}{b}$ and $\overline{r} = 1.0$ was a point of helical symmetry and the radial velocity was automatically zero), and Equation (12) yielded 10 equations for satisfying the normal induced velocity component on the inner helical vortex sheet. Due to the helical symmetry there were certain repeating coefficients and the total number of integrations required were 195. In addition, the symmetry occurring in the wake boundary sheet strength about the line of intersection reduced the number of unknowns to 15. Thus, 14 equations were obtained in the 15 unknowns. The 15th equation was that the sum of the strengths of the 20 vortex filaments be zero.

The nondimensional blade bound vortex strength was assumed to be adequately represented by the first 10 terms of Equation (16). Thus,

$$\frac{\Gamma}{2\pi R_o\ w\ \tan\ \varphi_o} = B_1 \sin \frac{\pi}{2}\ \overline{r} + B_3 \sin \frac{3\pi}{2}\ \overline{r} + \text{----} + B_{19} \sin \frac{19\pi}{2}\ \overline{r} \qquad (19)$$

The filament strengths were then simply the difference in this equation evaluated at the ends of the vortex sheet segment that the filament replaced.

COMPUTER RESULTS

The computer results are presented in Table 1 and in Figures 2 and 3. In Table 1 is listed the Fourier series coefficients of Equation (19) that were obtained from the simultaneous solution of the vortex filament equations for a two- and a four-bladed, lightly loaded shrouded propeller operating at an advance ratio of 1.356. In Figures 2 and 3, a plot of Equation (19) is compared with the results of the potential tank analysis presented in Gray's report[2]. The function $K(x)$ is used in this case for convenience, where

$$K(x) = \frac{b\ \Gamma}{2\pi R_o\ w\ \tan\ \varphi_o} \tag{20}$$

[2]Gray, op. cit. ante page 5.

TABLE 1

COEFFICIENTS APPEARING IN THE FOURIER SERIES REPRESENTATION
OF THE BLADE BOUND VORTEX STRENGTH FOR A TWO- AND A FOUR-BLADED
SHROUDED PROPELLER

$$\tan \varphi_o = 1.356$$

$$\frac{\Gamma}{2\pi R_o \; w \; \tan \varphi_o} = B_1 \sin \frac{\pi}{2} \bar{r} + B_3 \sin \frac{3\pi}{2} \bar{r} + \text{-----} + B_{19} \sin \frac{19\pi}{2} \bar{r}$$

Coefficient	Two Blades	Four Blades
B_1	+ 0.09089	+ 0.05305
B_3	- 0.00297	0.00697
B_5	+ 0.00103	0.00099
B_7	- 0.00048	0.00086
B_9	+ 0.00026	0.00028
B_{11}	- 0.00014	0.00024
B_{13}	+ 0.00007	0.00012
B_{15}	- 0.00003	0.00007
B_{17}	+ 0.00001	0.00005
B_{19}	0	0

24
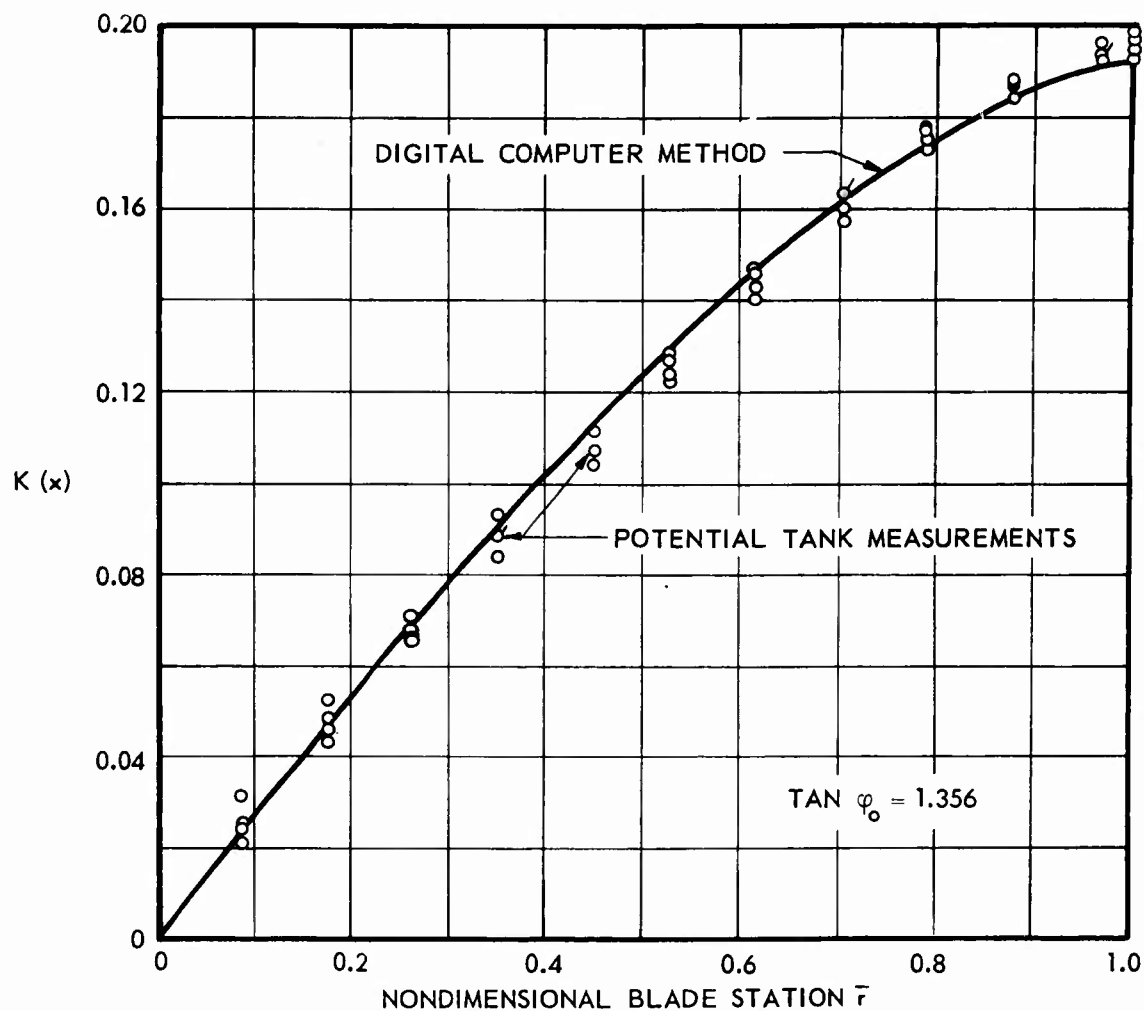
Figure 2. A Comparison of the Results of Two Methods of Determining the Variation in the Nondimensional Blade Bound Vortex Strength Distribution Function with Nondimensional Blade Radius for a Lightly Loaded, Single-Rotation, Two-Bladed Shrouded Propeller.
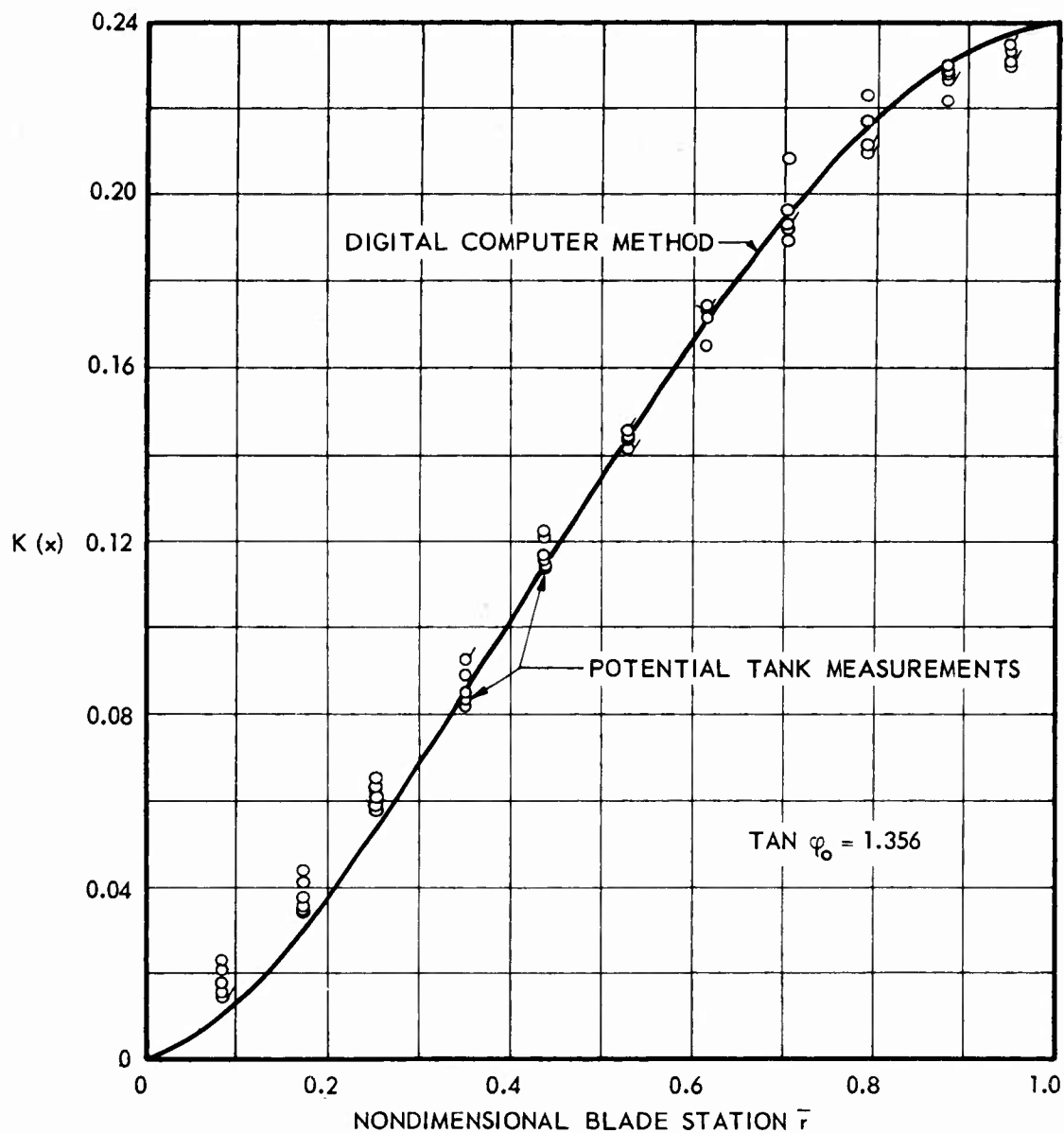
Figure 3. A Comparison of the Results of Two Methods of Determining the Variation in the Nondimensional Blade Bound Vortex Strength Distribution Function with Nondimensional Blade Radius for a Lightly Loaded, Single-Rotation, Four Bladed Shrouded Propeller.

The accuracy of the results is not known since it is highly dependent on the number of finite vortex filaments used to approximate the vortex sheets. An estimate of the accuracy could be obtained by using twice the number of filaments in the analysis, but this was not considered in view of the extra time and funds required for its accomplishment. However, in view of the close agreement between the two methods, it is believed that the results are sufficiently accurate for design purposes.

EVALUATION

The initial comparison of the blade bound vortex strength distribution for the two-bladed shrouded propeller as determined by the computer analysis with that measured on the potential tank model showed a difference of about seven per cent at all blade stations, the computer quantities being the higher. This was believed to be excessive in view of the estimated accuracy of the analyses so that a re-evaluation of the potential tank data was undertaken. A small computational error was discovered in the quantity that was used to nondimensionalize the potential tank measurements for the two-bladed propeller case. These results were corrected and are plotted in Figure 2 for the comparison purposes. A similar check of the four-bladed propeller case did not show a similar error, so that this data is as presented before.

The comparison between the computed nondimensional blade bound vortex distribution and the measurements obtained from the potential tank model is very good for the two-bladed shrouded propeller. As may be seen from Figure 2, the difference is about 2 per cent below the mean measured value at the blade tip. Since the potential measurements were made at the center of a two-turn helical model, it was felt that the end effects of the model might be causing this small difference. Accordingly, the integrations in the computer method were limited to the same length and the Fourier series coefficients were re-determined. It was found that the effect was in the right direction but was very small, bringing about an increase of 0.2 per cent in B_1 and about 0.5 per cent in B_{17}. There-

28

fore, inasmuch as the estimated measurement error for the potential tank results was ± 2 per cent of the maximum readings, it was felt that the agreement between the two methods was sufficient and further inquiry into this small difference was not warranted. However, the difference may be attributed to small errors in model construction and/or to the approximation introduced into the computer method by replacing a vortex sheet with a finite number of finite strength vortex filaments.

As may be seen from Figure 3, the difference in the computed blade bound vortex distribution and the measurements from the potential tank model for the four-bladed shrouded propeller is also about 2 per cent at the blade tip, but is considerably more near the blade root. Inasmuch as the four-bladed potential model was much more difficult to construct and therefore of less accuracy than the two-bladed model, it is believed that this increased percentage difference is due primarily to model construction errors and to the small warpage that occurred in the model as it absorbed the electrolyte.

In view of the success achieved with the computer method and from past experience of the difficulties encountered in the construction of potential tank models of the wakes of shrouded propellers, it is concluded that the computer method is the more efficient means of obtaining the desired results.

From Table 1, it may be seen that for the cases investigated, the first four coefficients of the series representation of the blade bound vortex distribution are sufficient for engineering design purposes. The use of this form of representation has two primary advantages. The first has been discussed previously and allows the boundary conditions on the

29

distribution to be expressed more easily. The second advantage would appear in the presentation of the results if the present work were to be extended to generate the necessary optimum parameters for design purposes by performing the computations for a range of advance ratios and numbers of blades. Previous analyses for free[4] and ducted[1] propellers have presented a family of curves or a series of tables for the nondimensional blade bound vortex distribution versus nondimensional blade radius (similar to Figures 2 and 3) for various values of a parameter λ which is the tangent of the helix angle of the blade tip vortex filament. For values of λ other than those presented in the reports, an interpolation must be performed. However, if the sine series representation is used, it is believed that the coefficients may be plotted as a function of advance ratio and an explicit expression of four or five terms may then be obtained which will yield the required distribution versus blade station by a relatively simple calculation. This will reduce the number of curves or charts required for adequate data presentation and should also require a fewer number of advance ratios for which the complete computer analysis must be run. This is a particular advantage in that about 8 to 10 hours of computing time is required for each run. It thus appears that a very real savings could be obtained by use of the series representation.

The analysis presented herein is applicable only to lightly loaded shrouded propellers. In the case of the _free_ propeller, the lightly loaded analysis was extended[4] to the heavily loaded case by a simple

---

[4]T. Theodorsen, _Theory of Propellers_, McGraw-Hill Book Company, Inc., New York, 1948.

[1]Tachmindji, op.cit. ante page 5.

30

redefinition of one of the parameters. The extension to the heavily loaded

shrouded propeller does not appear to be as simple because of the addi-

tional compatibility requirement between the inner helical vortex sheet,

the boundary vortex sheet, and the discontinuity in induced velocity as

the boundary sheet is crossed. This requirement was neglected in the

present analysis and therefore restricts the results obtained from this

and similarly restricted analyses to those cases in which the induced

velocity is small in comparison with the free-stream velocity. If there

is no urgent need for the lightly loaded design parameters in the near

future, it is suggested that this approach be discontinued and any further

efforts be directed toward an analysis of the heavily loaded case, using

the same methods presented herein but including the additional condition

on the wake boundary vortex sheet.

It was felt that a comparison between the method of this report and

that of Tachmindji[1] would be worthwhile. Therefore, the nondimensional

blade bound vortex strength distribution for a four-bladed shrouded pro-

peller operating at an advance ratio of one-third was calculated and the

comparison is shown in Figure 4. It was expected that better agreement

between the two methods would be obtained. Limitations on time and funds

did not permit further investigation of the differences shown.

As an additional comparison, the distribution for an infinitely

bladed shrouded propeller was calculated using an expression given by

Theodorsen.[4] This is also shown in Figure 4.

---

[1]Tachmindji, op. cit. ante page 5.

[4]Theodorsen, op. cit. ante page 30.

31
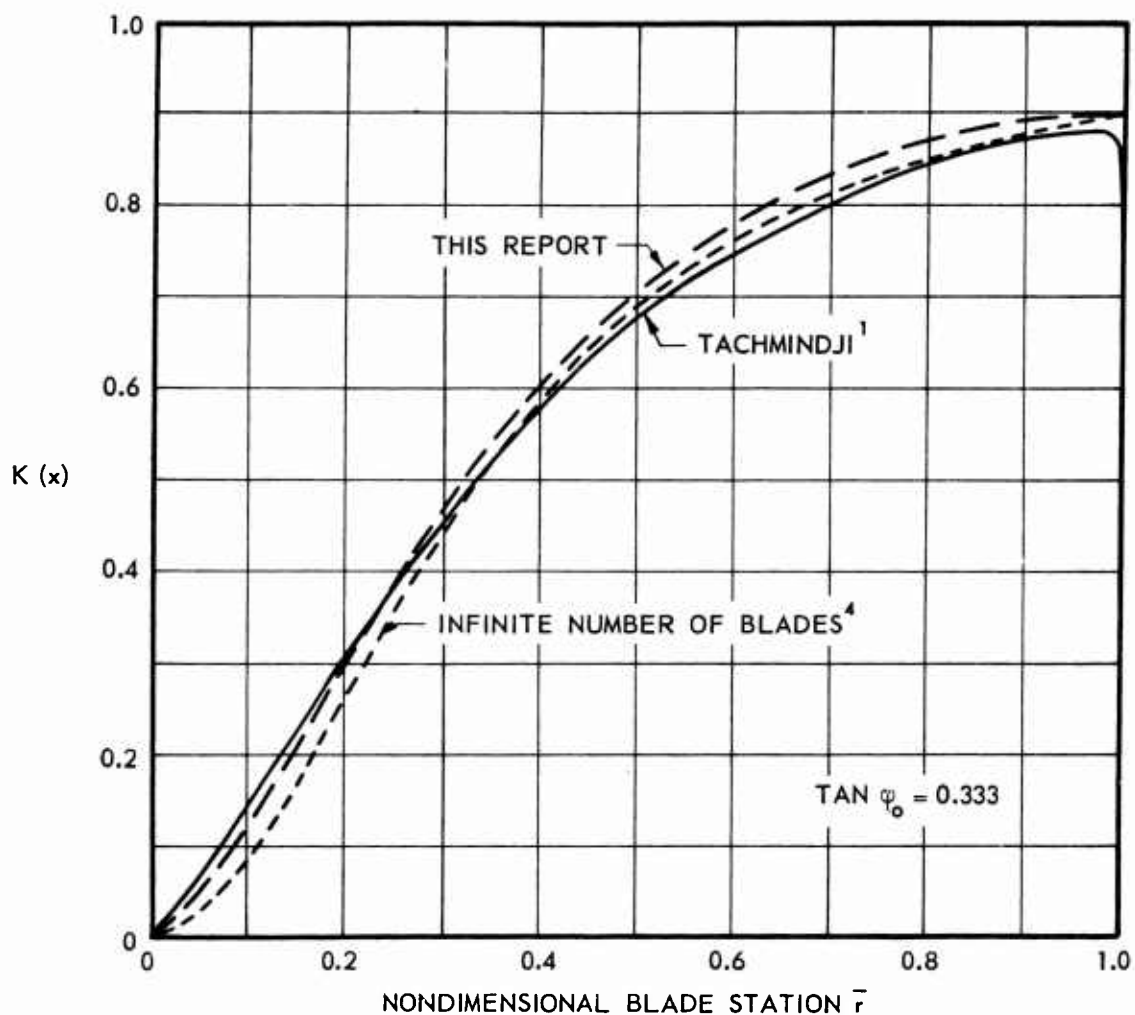
Figure 4. Comparison of Two Methods of Calculating the Nondimensional Blade Bound Vortex Distribution for a Lightly Loaded, Single-Rotation, Four-Bladed Shrouded Propeller and the Theoretical Distribution for an Infinitely Bladed Propeller.

[1] Tachmindji, op. cit. ante page 5
[4] Theodorsen, op. cit. ante page 30

32

DISTRIBUTION

USCONARC	(2)
First US Army	(1)
Second US Army	(1)
Third US Army	(1)
Fourth US Army	(1)
Fifth US Army	(1)
Sixth US Army	(2)
US Army Infantry Center	(1)
USA Command & General Staff College	(1)
Army War College	(1)
US Army Arctic Test Board	(1)
US Army Cold Weather and Mountain School	(1)
US Army Aviation School	(2)
US Army Armor Board	(1)
US Army Aviation Board	(2)
US Army Aviation Test Office	(1)
Deputy Chief of Staff for Logistics, DA	(4)
Deputy Chief of Staff for Military Operations, DA	(1)
ORO, Johns Hopkins University	(1)
ARO, OCRD	(1)
Office of Chief of R&D	(1)
ARO, Durham	(1)
Naval Air Test Center	(2)
US Army Chemical Corps Board	(1)
US Army Ordnance Missile Command	(1)
Ordnance Board, USA	(1)
Quartermaster Board, USA	(2)
Quartermaster Research and Engineering Command, USA	(1)
Quartermaster Field Evaluation Agency, USA	(2)
US Army Signal Board	(1)
Chief of Transportation, DA	(6)
US Army Transportation Combat Development Group	(1)
US Army Transportation Board	(2)
US Army Transportation Materiel Command	(20)
US Army Transportation Training Command	(1)
US Army Transportation School	(3)
US Army Transportation Research Command	(32)
US Army Engineer Waterways Experiment Station	(1)
USATRECOM Liaison Office, Wright-Patterson AFB	(1)
USATRECOM Liaison Officer, USAR&D Liaison Group (9851 DU)	(1)
TC Liaison Officer, USAERDL	(1)
USATRECOM Liaison Officer, Detroit Arsenal	(1)
US Army Transportation Terminal Command, Atlantic	(1)

U. S. Army Transportation Terminal Command, Pacific	(3)
USA TC Liaison Officer, Airborne and Electronics Board	(1)
US Army, Europe (Rear)/Communications Zone	(2)
Hq USATDS	(1)
US Army, Pacific	(1)
US Army, Alaska	(3)
Eighth US Army	(2)
US Army Transportation Agency, Japan	(1)
US Army, Ryukyu Islands/IX Corps	(1)
US Army, Hawaii	(3)
US Army Caribbean	(2)
Allied Land Forces Southeastern Europe	(2)
Air Research & Development Command	(1)
APGC(PGTRI), Eglin AFB	(1)
WADD(WWAD-Library)	(1)
Air University Library	(1)
Hq USAF (AFDFD)	(1)
Air Force Systems Command	(3)
Chief of Naval Research	(1)
Bureau of Naval Weapons	(7)
Asst. Chief for R&D (OW), Navy	(1)
US Naval Postgraduate School	(1)
David Taylor Model Basin	(1)
Hq, US Marine Corps	(1)
Marine Corps Schools	(3)
Marine Corps Liaison Officer, USA Transportation School	(1)
US Coast Guard	(1)
National Aviation Facilities Experimental Center	(10)
NASA, Washington, D. C.	(6)
George C. Marshall Space Flight Center, NASA	(4)
Langley Research Center, NASA	(3)
Ames Research Center, NASA	(1)
Lewis Research Center, NASA	(1)
Library of Congress	(2)
US Army Standardization Group, U.K.	(1)
US Army Standardization Group, Canada	(1)
Canadian Army Liaison Officer, USA Transportation School	(3)
British Joint Services Mission (Army Staff)	(3)
Armed Services Technical Information Agency	(10)
US Army Engineer Waterways Experiment Station	(1)
Institute of Aeronautical Sciences	(1)
Human Resources Research Office	(1)
Republic Aviation Corporation	(1)
Georgia Institute of Technology	(15)

Engineering Experiment Station, Georgia Institute of Technology, Atlanta, Georgia. AN INVESTIGATION OF A DIGITAL COMPUTER METHOD OF DETERMINING THE OPTIMUM DESIGN PARAMETERS OF SHROUDED PROPELLERS. - Robin B. Gray.

Report No. TCREC 61-124, October, 1961, 32 pp - figures - tables. Contract DA-44-177-TC-402. USATRECOM Task 9R38-11-009-12, Unclassified Report.

For the case of lightly loaded optimum shrouded propellers, the wake vortex pattern may be described as being made up of equal-pitch vortex filaments forming a helical inner sheet and a cylindrical outer sheet, the sheet strengths being the unknown quantities. For numerical analysis suitable for digital computers, the sheets were approximated by a number of finite strength vortex filaments. The relationship between the geometry and the filament strength was obtained from the Biot-Savart relation. Calculating points were chosen on the sheets, and a set of simultaneous equations in terms of the unknown filament strengths was obtained. The solution of these simultaneous equations yielded the required optimum blade bound vortex strength distributions.

The computer results for a two- and a four-bladed shrouded propeller operating at an advance ratio of 1.356 were compared with the measured results of a previous potential tank analysis. It was concluded that the digital computer analysis using a series representation of the blade bound vortex strength distribution was the more efficient approach.

Engineering Experiment Station, Georgia Institute of Technology, Atlanta, Georgia. AN INVESTIGATION OF A DIGITAL COMPUTER METHOD OF DETERMINING THE OPTIMUM DESIGN PARAMETERS OF SHROUDED PROPELLERS. - Robin B. Gray.

Report No. TCREC 61-124, October, 1961, 32 pp - figures - tables. Contract DA-44-177-TC-402. USATRECOM Task 9R38-11-009-12, Unclassified Report.

For the case of lightly loaded optimum shrouded propellers, the wake vortex pattern may be described as being made up of equal-pitch vortex filaments forming a helical inner sheet and a cylindrical outer sheet, the sheet strengths being the unknown quantities. For numerical analysis suitable for digital computers, the sheets were approximated by a number of finite strength vortex filaments. The relationship between the geometry and the filament strength was obtained from the Biot-Savart relation. Calculating points were chosen on the sheets, and a set of simultaneous equations in terms of the unknown filament strengths was obtained. The solution of these simultaneous equations yielded the required optimum blade bound vortex strength distributions.

The computer results for a two- and a four-bladed shrouded propeller operating at an advance ratio of 1.356 were compared with the measured results of a previous potential tank analysis. It was concluded that the digital computer analysis using a series representation of the blade bound vortex strength distribution was the more efficient approach.